J. Membrane Biol. 213, 19–29 (2006)
DOI: 10.1007/s00232-006-0037-y

The Journal of
Membrane
Biology

Functional Expression of Inward Rectifier Potassium Channels in Cultured Human Pulmonary Smooth Muscle Cells: Evidence for a Major Role of Kir2.4 Subunits

Brian P. Tennant, Yi Cui, Andrew Tinker, Lucie H. Clapp
Department of Medicine, BHF Laboratories, Rayne Institute, University College London, 5 University Street, London, WC1E 6JF, United Kingdom

Received: 1 June 2006/Revised: 4 October 2006

Abstract. Strong inwardly rectifying K^+ (K_{IR}) channels that contribute to maintaining the resting membrane potential are encoded by the Kir2.0 family (Kir2.1–2.4). In smooth muscle, K_{IR} currents reported so far have the characteristics of Kir2.1. However, Kir2.4, which exhibits unique characteristics of barium block, has been largely overlooked. Using patch-clamp techniques, we characterized K_{IR} channels in cultured human pulmonary artery smooth muscle (HPASM) cells and compared them to cloned Kir2.1 and Kir2.4 channels. In a physiological K^+ gradient, inwardly rectifying currents were observed in HPASM cells, the magnitude and reversal potential of which were sensitive to extracellular K^+ concentration. Ba^{2+} (100 μM) significantly inhibited inward currents and depolarized HPASM cells by ~10 m*V*. In 60 mM extracellular K^+, Ba^{2+} blocked K_{IR} currents in HPASM cells with a 50% inhibitory concentration of 39.1 μM at –100 m*V* compared to 3.9 μM and 65.6 μM for Kir2.1 and Kir2.4, respectively. Cloned Kir2.4 and K_{IR} currents in HPASM cells showed little voltage dependence to Ba^{2+} inhibition, which blocked at a more superficial site than for Kir2.1. Single-channel recordings revealed strong inwardly rectifying channels with an average conductance of 21 pS in HPASM cells, not significantly different from either Kir2.1 (19.6 pS) or Kir2.4 (19.4 pS). Reverse-transcription polymerase chain reaction detected products corresponding to Kir2.1, Kir2.2 and Kir2.4 but not Kir2.3. We demonstrate that cultured HPASM cells express K_{IR} channels and suggest both Kir2.1 and Kir2.4 subunits contribute to these channels, although the whole-cell current characteristics described share more similarity with Kir2.4.

Key words: Inward rectifier potassium channel — Pulmonary artery — Human — Kir2.4 — Patch clamp

Introduction

Strong inwardly rectifying K^+ (K_{IR}) channels have been described in many vascular and visceral tissues from different species (Quayle, Nelson & Standen, 1997; Nilius & Droogmans, 2001). These channels pass most current at potentials hyperpolarized to the K^+ equilibrium potential (E_K), though the small amount of outward current carried at voltages depolarized to this potential is enough to regulate the resting membrane potential (E_m) and to cause blood vessel dilatation in response to either raised extracellular (10–15 mM) K^+ (Quayle et al., 1997) or shear stress (Hoger et al., 2002). Since their initial identification in rat cerebral and coronary artery (Edwards, Hirst & Silverberg, 1988; Quayle et al., 1993; Knot, Zimmermann & Nelson, 1996), patch-clamp studies have reported strongly rectifying inward currents in isolated lung endothelial and bronchial smooth muscle cells (Voets, Droogmans & Nilius, 1996; Kamouchi et al., 1997; Snetkov & Ward, 1999; Michelakis et al., 2001; Hogg, McMurray & Kozlowski, 2002; Oonuma et al., 2002; Shimoda, Welsh & Pearse, 2002). Regardless of their origin within the cardiovascular system, K_{IR} currents recorded to date are potently blocked by micromolar external Ba^{2+} ions in a manner that is steeply voltage- and time-dependent (Quayle et al., 1993; Robertson, Bonev & Nelson, 1996; Bradley et al., 1999; Snetkov & Ward, 1999; Sakai et al., 2002; Oonuma et al., 2002).

The first two authors contributed equally to the work.

Correspondence to: L. H.Clapp; email: l.clapp@ucl.ac.uk

At the molecular level, the Kir2.0 subfamily almost certainly encodes the classical inward rectifiers found in the brain, heart and skeletal and vascular muscle (Quayle et al., 1997; Stanfield, Nakajima & Nakajima, 2002). These channels form as tetramers of subunits that have only two membrane-spanning regions, between which is the H5 loop responsible for potassium selectivity. Four isoforms have been identified, Kir2.1, −2.2, −2.3 and −2.4 (Stanfield et al., 2002). The properties of the first three have been extensively characterized, while that of Kir2.4 has been much less studied, probably due to its restricted expression. Apart from Kir2.4, all subunits show the blueprint of voltage- and time-dependent block with Ba^{2+} (Bradley et al., 1999; Hughes et al., 2000; Preisig-Muller et al., 2002; Schram et al., 2002). In smooth muscle, the evidence so far indicates that Kir2.1 might encode K_{IR} currents in both native and cultured cells. Reverse-transcription polymerase chain reaction (RT-PCR) analysis demonstrated the presence of Kir2.1, but not Kir2.2 and Kir2.3, in rat cerebral, coronary and mesenteric artery; canine colonic smooth muscle; and human bronchial smooth muscle (Bradley et al., 1999; Oonuma et al., 2002; Flynn et al., 1999), although Kir2.4 was not examined in these studies. Moreover, expression of Kir2.1 cloned from rat mesenteric vascular smooth muscle cells into *Xenopus* oocytes produced K_{IR} currents that resembled those observed in native vascular smooth muscle cells (Bradley et al., 1999).

The aim of the present study was to identify and examine the properties of K_{IR} channels in cultured human pulmonary artery smooth muscle (HPASM) cells and determine the expression of members of the Kir2.0 subfamily. Here, we show that three out of the four Kir2.0 subunits are expressed at the transcriptional level in cultured HPASM cells and that the properties of the K_{IR} currents recorded in these cells most closely resemble those of Kir2.4, although other subunits are likely to contribute. We thus provide the first functional evidence for a role of Kir2.4 outside the central and peripheral nervous systems.

Materials and Methods

Cell Culture

Cultured HPASM cells were obtained from Clonetics (fourth passage; San Diego, CA) and plated in smooth muscle growth medium (SmGM, Clonetics) supplemented with gentamicin (50 μg/ml), human epidermal (0.5 μg/ml) and fibroblast (1.0 μg/ml) growth factors, insulin (5 μg/ml) and 5% fetal bovine serum. Cells were grown at 37°C in a humidified atmosphere of 5% CO_2 as described (Cui et al., 2002). After reaching confluence, cells were scratched from the dish by treatment with accutase (TSC Biologicals, Buckingham, UK) and transferred to T75 flasks for further passage. Smooth muscle cells were characterized by immunohistochemical staining using a mouse anti-α-actin monoclonal antibody (Boehringer-Mannheim, Mannheim, Germany). For electrophysiological experiments, cells (up to passage 8) were plated onto coverslips in six-well plates at a density of 30,000/well and at 24 h the growth medium was replaced by serum-free Dulbecco's modified Eagle medium (DMEM, without antibiotics) to inhibit cell proliferation. Experiments were performed on cells starved of serum for at least 24 h. HEK-293 cells (human embryonic kidney cell line) were cultured in a humidified atmosphere in 5% CO_2 in minimal essential medium supplemented with Earle's salts, 10% L-glutamine, 10% fetal bovine serum and 1% penicillin/streptomycin (from a stock of 10,000 units/ml penicillin and 1 mg/ml streptomycin).

Transfection and Generation of Monoclonal Stable Lines

Mouse Kir2.1 cDNA was a kind gift from Lilly Jan (Howard Hughes Medical Institute, University of California, San Francisco, CA), and rat Kir2.4 cDNA was a kind gift from Diomedes Logothetis (Mount Sinai School of Medicine, New York, NY). HEK-293 cells were transfected with Kir2.1 and Kir2.4 subcloned into pcDNA3 vectors (Invitrogen, La Jolla, CA) using Lipofectamine (Life Technologies, Bethesda, MD) according to the manufacturer's instructions (Cui et al., 2001). Stable cell lines were established using the appropriate antibiotic selection (G418 for Kir2.1, Zeocin for Kir2.4) as detailed previously (Giblin, Leaney & Tinker, 1999). In some experiments, HEK-293 cells were transiently transfected with Kir2.1 and green fluorescence protein cDNAs and successfully transfected cells were identified by epifluorescence.

Molecular Biology

To identify K_{IR} channels in HPASM cells by molecular methods, RT-PCR was used. For mRNA isolation, HPASM cells were grown in 3 × T175 flasks to confluence and washed twice with cold phosphate-buffered saline (made in diethylpyrocarbonate H_2O). Using an RNA isolation kit (Fast-track2.0, Invitrogen) and following the manufacturer's instructions, polyA RNA was isolated using the oligo dT cellulose column provided. Synthesis of cDNA was carried out using 1 μl polyA RNA (100 ng) and oligo dT primers and following the manufacturer's instructions (cDNA cycle kit, Invitrogen). For PCR, 2 μl of cDNA was used in a 50 μl reaction and the following added: 5 μl PCR buffer (x10, containing 1.5 mM $MgCl_2$, Boehringer Mannheim), 1 μl deoxynucleoside-5′-triphosphate solution (containing 25 mM of each deoxynucleotide triphosphate), 1 unit *Taq* DNA polymerase (Boehringer-Mannheim) and 1 μM of each specific primer. Primers were as follows: Kir2.1 (GenBank accession AF153819) forward (5′-TCTTGGGA ATTCTGGTTTGC-3′), reverse (5′-TGGGAGCCTTGTGGTTCT AC -3′), Kir2.2 (NM_021012) forward (5′-TCGATGTGGGCTTC GACAA -3′), reverse (5′-GTAGAGGGCACCTCATAGG -3′), Kir2.3 (U07364) forward (5′-AACCGCTTCGTCAAGAAGAA-3′), reverse (5′-GATACACCAGAAGAGGAGGC-3′), Kir2.4 (AF081466) forward (5′-AATGGGGTGGAAACAGAAGATG-3′), reverse (5′-GTCTATACCATTGGCTTCTCAC-3′). The cycling conditions were 94°C for 30 s, 54°C for 30 s and 74°C for 30 s for 35 cycles and final extension for 10 min. As a negative control, 2 μl of the RT-PCR product synthesized in the absence of AMV-Transcriptase was used as a template. PCR products were electrophoresed on a 1.3 % agarose gel. The sequence of PCR products was confirmed by sequencing using a dye terminator kit (Applied Biosciences, Foster City, CA) and an automatic sequencer (ABI377; Perkin-Elmer, Foster City, CA). As a positive control for Kir2.3, human Kir2.3 cDNA (Gene Service, Cambridge, UK) was

amplified under the same conditions, using only 12.5 pg of cDNA as template.

Electrophysiological Recording

Currents and membrane potentials were recorded in the whole-cell and cell-attached configurations of the patch-clamp technique using an Axopatch 200B amplifier (Axon Instruments, Foster City, CA). Current signals were filtered at 1–2 kHz (8-pole low-pass Bessel), digitized at 5 kHz using the Digidata 1200 interface and saved on a computer for later analysis. Patch pipettes from either thin- (1.7 mm optical density [OD]) or thick- (1.5 mm OD) walled borosilicate glass capillaries (Clark Electromedical, Pangbourne, UK) were pulled and fire-polished using a DMZ-universal puller (Zietz Instruments, Munich, Germany). Pipettes had resistance of 2–4 MΩ for whole-cell recordings and 6–12 MΩ for single-channel recordings when filled with electrolyte solution. Electrode capacitance was reduced by coating pipettes with a parafilm/mineral oil suspension and compensated electronically. Series resistance during whole-cell recording was compensated to at least 75% by the amplifier.

Data Analysis

Electrophysiological data were analyzed using pClamp (version 6, Axon Instruments), SATORI v3.2 (Intracel, Coventry, UK) and Origin (version 6 & 7; Microcal Software, Northampton, MA) software. Values are given as means ± standard error of the meant (SEM), and n indicates the number of cells. For current-voltage (I-V) relationship graphs, current was measured during the final 10 ms of each voltage step and averaged for each cell. The barium concentration-response curves were analyzed and fitted using the sigmoidal fitting routine in Origin. The drug concentration at which half-maximal current is inhibited (K_D) was obtained using the logistical function.

$$\frac{I_{Ba}}{I_{Con}} = \frac{1}{1+(X/K_D)^n} \quad (1)$$

where I_{Ba} is the current in the presence of barium, I_{Con} is the current in control, X is the extracellular Ba^{2+} concentration and n is the slope factor (Hill coefficient). Statistical significance was assessed using a paired or unpaired Student's t-test. $P < 0.05$ was considered statistically significant.

Solutions and Drugs

For whole-cell recordings in HPASM cells, the standard bath solution was an extracellular physiological salt solution (PSS) containing (mM) 137 NaCl, 5 KCl, 0.4 KH_2PO_4, 0.3 NaH_2PO_4, 2 $NaHCO_3$, 1 $MgCl_2$, 1.8 $CaCl_2$, 10 4-(2-hydroxyethyl)-1-piperazineethanesulfonic acid (HEPES) and 5.5 glucose (pH 7.4 with NaOH). To assess the voltage dependence of Ba^{2+} block and the effect on the reversal potential, whole-cell experiments in HPASM and HEK-293 cells were conducted in a high-potassium bath solution (60 mM K^+), which was made by replacing NaCl in the PSS with an equimolar concentration of KCl. The basic pipette solution contained (mM) 130 KCl, 1 $MgCl_2$, 1 ethyleneglycoltetraacetic acid (EGTA), 15 HEPES and 1 adenosine triphosphate-Na_2 (ATP). The pH of the solutions was adjusted to 7.20 with KOH, to give a final K^+ concentration of 140 mM. For single-channel recordings, the pipette and bath solution was (mM) 140 KCl, 1.0 $MgCl_2$, 1 EGTA and 10 HEPES (pH 7.2 NaOH). $BaCl_2$, ATP and glibenclamide were obtained from Sigma (Poole, UK).

Results

Whole-Cell Inward Rectifier Currents in Physiological K^+ and High (60 mM) K^+ Gradient

Cultured HPASM cells were perfused with PSS containing 5 mM K^+ and dialyzed with a pipette solution containing 140 mM K^+. Under these conditions, application of 300-ms voltage steps from −150 to + 40 mV at a holding potential of −60 mV evoked both inward and outward currents (Fig. 1A). Upon application of the K_{IR} channel blocker Ba^{2+} (100 μM), only currents activated in the inward direction were significantly inhibited (Fig. 1A, lower panel). Figure 1B shows mean I-V relationships of currents obtained from experiments similar to that shown in Figure 1A. Inward currents measured at −120 mV were reduced by 70% from −66.3 ± 10.7 pA under control conditions to −19.4 ± 3.21 pA ($n = 8$, $P < 0.01$) in the presence of Ba^{2+}. Such effects were fully reversible upon washout of Ba^{2+} (Fig. 1B). In contrast, outward currents evoked by voltages positive to −30 mV were essentially unaffected by the same concentration of Ba^{2+} (Fig. 1B) such that currents measured at + 40 mV were 56.9 ± 10.6 pA under control conditions and 62.8 ± 6.8 pA ($P > 0.05$ $n = 8$) in the presence of Ba^{2+}. Plotting the Ba^{2+}-sensitive current revealed the characteristics of inward rectification of the current, having a reversal potential of −74.4 ± 2.2 mV ($n = 8$) in a 5/140 mM K^+ gradient (Fig. 1C). This is close to the calculated E_K under these conditions of −82 mV. Since K_{IR} channels are highly selective for K^+ ions, showing a positive shift in the I-V relationship and an increase in conductance of the channel with increasing concentration of extracellular K^+, we further characterized currents by performing experiments with 60 mM K^+ in the bathing solution. Under these conditions, the same voltage-clamp protocols as above were applied. As expected, bigger inward currents were evoked at hyperpolarized potentials averaging −378.0 ± 78.4 pA at −120 mV ($n = 6$). Upon application of Ba^{2+} (30 μM), currents were significantly inhibited to −232.1 ± 41.5 pA ($P < 0.01$, $n = 6$). The mean I-V relationship of the Ba^{2+}-sensitive current is shown in Figure 1C, giving a reversal potential of −22.4 ± 3.0 mV ($n = 11$) for the current, close to the calculated E_K of −21 mV under these conditions. Similarly, outward currents were not affected (360.6 ± 72.8 pA at + 40 mV under control conditions and 381.8 ± 77.7 pA in the presence of Ba^{2+}, $P > 0.05$, $n = 6$). In addition, the K_{ATP} channel blocker glibenclamide (10 μM) had no effect on the Ba^{2+}-sensitive currents (*data not shown*). Thus, the Ba^{2+}-sensitive current shifted when K^+ was altered and reversed near the expected E_K, indicating that currents were indeed through K^+-selec-

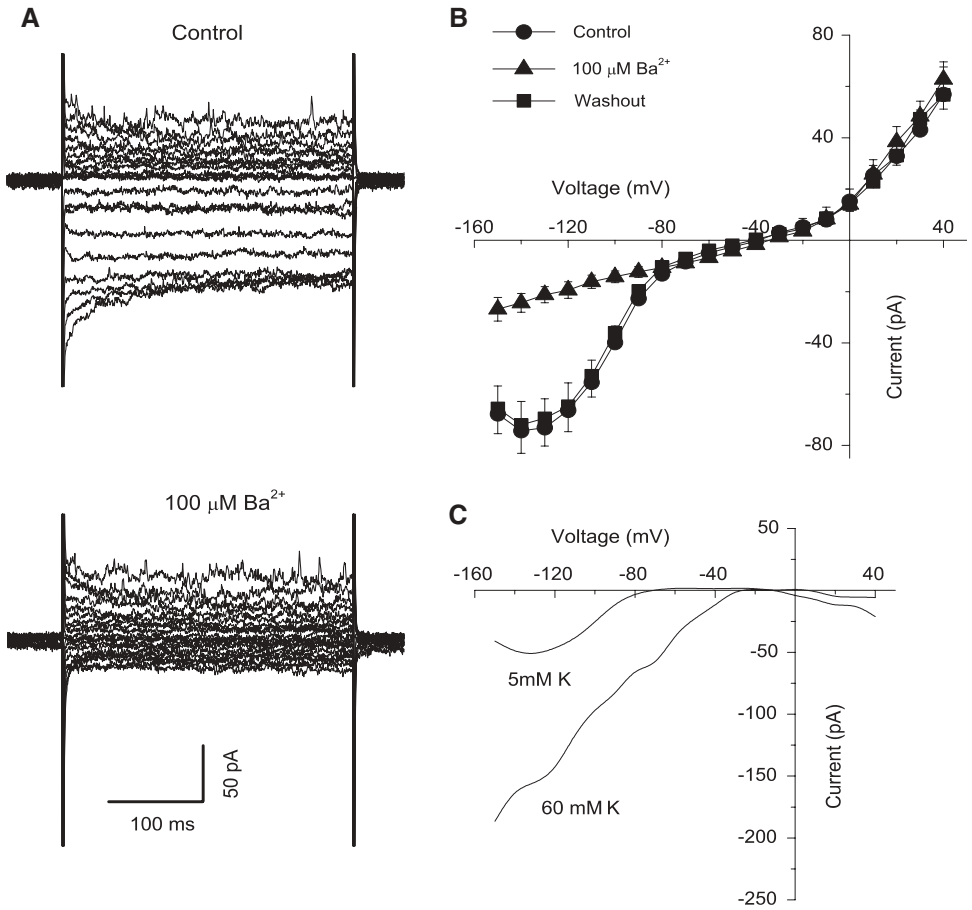

Fig. 1. (*A*) Effects of Ba^{2+} (100 μM) on currents evoked by 300-ms voltage steps from −150 to + 40 m*V* at a holding potential of −60 m*V* in a single HPASM cell. (*B*) Mean *I-V* curves obtained from a series of experiments ($n = 8$) similar to above, obtained under control conditions, in the presence of Ba^{2+} and following washout. (*C*) *I-V* curves of Ba^{2+}-sensitive currents recorded in physiological K^+ (5/140 mM) and high-K^+ (60/140 mM) gradients. Data are expressed as mean ± SEM.

tive channels. K_{IR} channels have been proposed to contribute to the maintenance of resting membrane potential, so their potential role was examined in current clamp ($I = 0$) mode in cells bathed in PSS. Under these conditions, cells had a resting potential of −44.3 ± 4.4 m*V* ($n = 7$). Following application of 100 μM Ba^{2+}, the resting potential became significantly more depolarized, to −34.7 ± 3.0 m*V* ($P < 0.05$ paired *t*-test). These results indicate that K_{IR} currents contribute to the maintenance of resting membrane potential in cultured HPASM cells.

Characteristics of Ba^{2+} Block in HPASM

To determine the nature of the Ba^{2+} block, inhibition of the current was examined over a range of Ba^{2+} concentrations (1–1,000 μM) in the presence of 60 mM extracellular K^+. Figure 2A shows families of inward currents activated by 300-ms pulses from −150 to 0 m*V* in an increment of 10 m*V*. In this and most cells, inward currents were typically noisy at membrane potentials at or below −80 m*V*. Application of Ba^{2+} blocked inward current above a concentration of 1 μM, though block showed little or no time dependence in this or any other HPASM cell; but it did reduce current noise seen at negative potentials. Figure 2B summarizes results of experiments from nine HPASM cells where the average steady-state *I-V* relationship in the presence of increasing concentrations of Ba^{2+} has been plotted. The concentration dependence of the Ba^{2+} block was assessed by plotting mean values of the fractional current remaining in the presence of Ba^{2+}. Using nonlinear least squares optimization and fitting data to equation 1, the extrapolated value for K_D at −100 m*V* was 39.1 μM (Fig. 2C), although it should be noted that the Hill coefficient of the sigmoidal fit was shallow (slope = 0.37). One possible explanation is that whole-cell current contains at least two populations of K_{IR} channels with distinct Ba^{2+} sensitivities. Among the Kir2.0 family, Ba^{2+} block is most sensitive in Kir2.2, followed by Kir2.1, Kir2.3 and Kir2.4, with the 50% inhibitory concentration (IC_{50}) being ~0.5, 3.2, 10–18 and 70–116 μM, respectively (Topert et al., 1998; Hughes et al., 2000; Liu et al., 2001; Preisig-Muller et al., 2002; Schram et al., 2002). Thus, based on the characteristics of the Ba^{2+} block of K_{IR} currents in cultured HPASM cells, this would suggest a major contribution from Kir2.4. We therefore sought to make comparisons

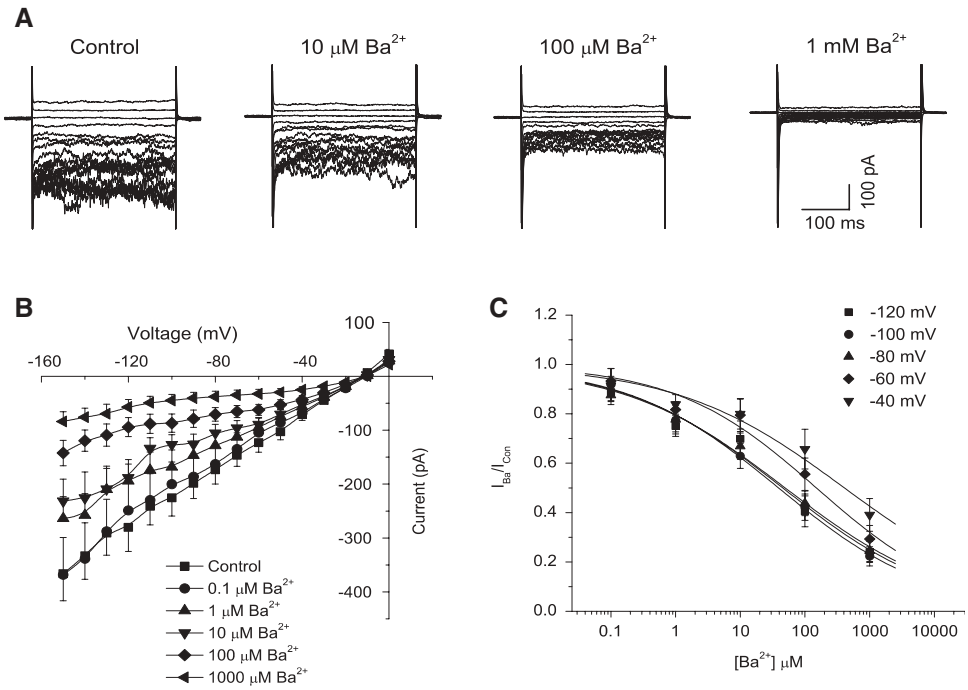

Fig. 2. Concentration dependence of the Ba^{2+} block of K_{IR} currents in HPASM cells. (*A*) Effects of Ba^{2+} on a family of currents evoked by 300-ms voltage steps from –150 to 0 m*V* at a holding potential of –20 m*V*. (*B*) Mean *I-V* relationships of steady-state current recorded in the absence and presence of increasing concentrations of Ba^{2+} ($n = 9$). (*C*) Concentration-response curves for the Ba^{2+}-induced block measured at various potentials (–120 to –40 m*V*). *Solid lines* represent best fit of the data to equation 1. Values for the IC_{50} and the slope factor (n) were 45.2 μM ($n = 0.36$), 39.1 μM ($n = 0.37$), 49.4 μM ($n = 0.35$), 150.0 μM ($n = 0.40$) and 407.6 μM ($n = 0.33$) at –120, –100, –80, –60 and –40 m*V*, respectively.

with Kir2.1 and Kir2.4 subunits stably expressed in HEK-293 cells.

Comparisons of Ba^{2+} Block of Kir2.1 and Kir2.4 Stably Expressed in HEK-293 Cells

The effect of Ba^{2+} (0.03–10,000 μM) was studied under similar experimental conditions to the above against currents activated in a 60/140 K^+ gradient. In cells expressing Kir2.1, Ba^{2+} significantly blocked inward currents in a manner that was visibly time-dependent (Fig. 3A), with little block of the instantaneous inward current at 10 or 100 μM but almost complete block of the steady-state current at the end of the voltage step. By comparison, currents carried by Kir2.4 were weakly affected by Ba^{2+} at 10 μM, showed no time dependence to the block and required mM Ba^{2+} to produce near full block in the inward direction and partial (50%) in the outward direction. Figure 3B summarizes the average steady-state *I-V* relationships for Kir2.1 and Kir2.4, where current for each subunit is plotted relative to that activated at −150 m*V*. The *I-V* relationships show a similar profile of steep inward rectification, although Kir2.4 passes significantly ($P < 0.05$, $n = 6$–12) more outward current at positive potentials, whether this is given in absolute terms (150 ± 34 *vs.* 70 ± 7 pA) or relative to control current at −150 m*V* (0.05 ± 0.01 *vs.* 0.01 ± 0.001) for the current measured at + 20 m*V*. As expected for a K^+ current, the reversal potential of the current blocked by 100 μM Ba^{2+} was 18.6 ± 2.8 m*V* ($n = 8$) and 21.8 ± 2.3 m*V* ($n = 7$) for Kir2.1 and Kir2.4, respectively. The concentration dependence of the Ba^{2+} block for the two subunits was assessed by plotting mean values of fractional current and fitting the data to equation 1 (Fig. 3C). Using this approach gave K_D values at −100 m*V* of 3.9 μM and 65.6 μM for Kir2.1 and Kir2.4, respectively.

Voltage Dependence of the Ba^{2+} Block

The effect of membrane potential on the K_D of barium block was compared for Kir2.1 and Kir2.4 (Fig. 4A). In cells expressing Kir2.1, K_D increased ~10-fold between that calculated at −100 and −40 m*V*, as evidenced by the rightward shift in the dose-response curves. By contrast, the K_D in Kir2.4-expressing cells showed much less dependence on voltage, increasing only threefold over the same voltage range. In HPASM cells, the effect of voltage appeared to be intermediate between Kir2.1 and Kir2.4, though at −60 m*V* and above the K_D became more steeply dependent on voltage (Fig. 2C). The

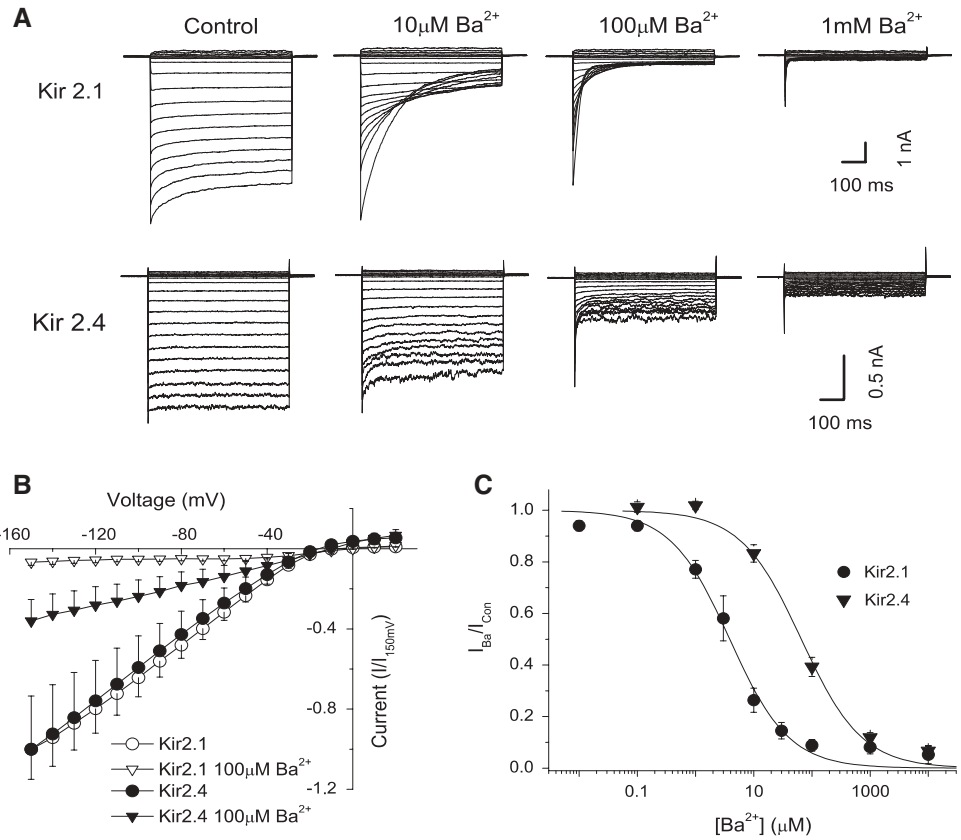

Fig. 3. Whole-cell characteristics of Kir2.1 and Kir2.4 stably expressed in HEK-293 cells showing differential sensitivity to Ba^{2+}. (*A*) Effects of increasing concentration of Ba^{2+} on a family of currents evoked by 600-ms voltage steps from −150 to + 20 m*V* at a holding potential of −20 m*V* in a 60/140 K^+ gradient. (*B*) Mean *I-V* relationships of steady-state current plotted relative to control current at –150 m*V* recorded in the absence (○) and presence (*σ*) of 100 μM Ba^{2+} for currents expressed by Kir2.1 (n = 6–12) (*closed symbols*) and Kir2.4 (n = 6) (*open symbols*). (*C*) Concentration-response curves for the Ba^{2+}-induced block shown for currents recorded at −100 m*V*. Values for the dissociation constant (K_D) and the slope factor (n) were derived by the fit to equation 1. For Kir2.1, K_D was 3.9 μM (n = 0.85) at −100 m*V* and the corresponding value for Kir2.4 was 65.6 μM (n = 0.83).

voltage dependence of the block can be investigated by the quantitative approach used by Woodhull (1973). The basic assumption is that there is a single site accessible to a blocker with a valence of z, lying at a fractional distance, δ, into the transmembrane field. Data obtained from Figures 2C and 4A were fitted to equation 2, where the ratio of the current in the presence of the blocker over the control current (I/I_{Con}) is plotted as a function of voltage (V) at a single blocker concentration (B) to extrapolate values for

$$\frac{I}{I_{Con}} = \frac{1}{1+\{[B]/K_D(0)\}e^{z\delta(FV/RT)}} \quad (2)$$

(1) $K_D(0)$ being the dissociation constant at 0 m*V;* δ, *F, R* and *T* having their usual meanings; and *RT*/*F* being 25.2 m*V* at 20°C. Using this approach, the best fit parameters at a blocking concentration of 100 μM Ba^{2+} were $K_D(0)$ = 142 ± 23 μM, 197 ± 18 μM, 337 ± 45 μM and δ = 0.38 ± 0.04, 0.15 ± 0.02 and 0.21 ± 0.03 for Kir2.1 (n = 10), Kir2.4 (n = 9) and HPASM (n = 9) cells, respectively (Fig. 4B). The δ value for Kir2.1 was significantly different from that for Kir2.4 and HPASM ($P < 0.001$). Varying the Ba^{2+} concentration by 10-fold gave similar values for δ, though this altered $K_D(0)$ by three- to fourfold (*see* Fig. 4 legend). These data suggest that Ba^{2+} appears to act at a more superficial site in HPASM cells than would be predicted if native K_{IR} channels were composed of just Kir2.1 subunits and that values for $K_D(0)$ and δ are closer to those obtained for channels made up of cloned Kir2.4 subunits.

Single-Channel Recordings

The properties of the Ba^{2+}-sensitive currents in HPASM cells were investigated in the cell-attached configuration and compared with HEK-293 cells expressing cloned Kir2.1 or Kir2.4 channels. Recordings were made in symmetrical K^+ (140/140 mM). Additionally, we made recordings of Kir2.4 in the presence of Ba^{2+} (300 μM in the patch pipette). This was done because the only report to date describing a conductance for Kir2.4 by single-channel

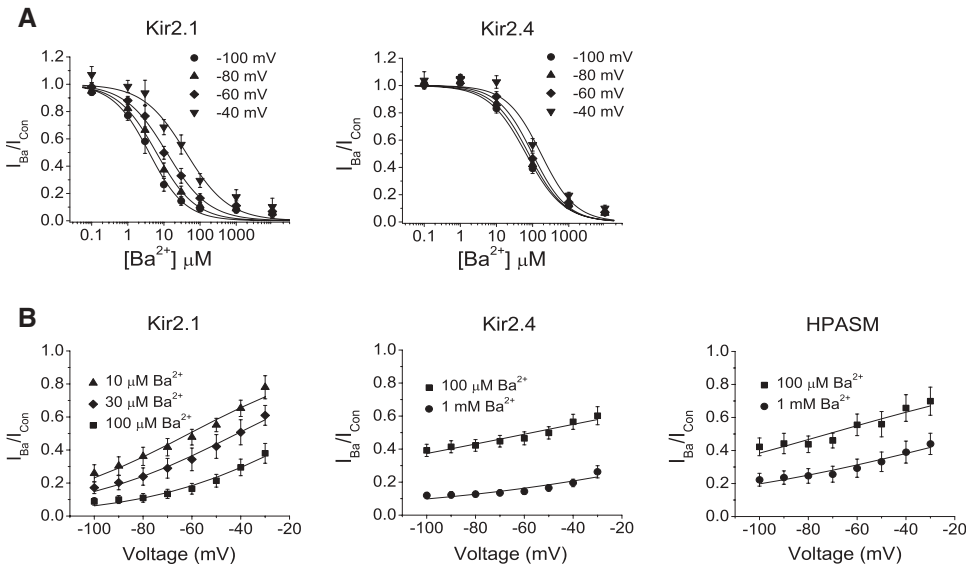

Fig. 4. Voltage dependence of the Ba^{2+}-induced block in cells expressing Kir2.1 or Kir2.4 compared with endogenous K_{IR} currents expressed in HPASM cells. (*A*) Concentration-response curves for the Ba^{2+}-induced block of inward currents activated at various potentials from −100 to −40 m*V* by Kir2.1 and Kir2.4. *Solid lines* represent best fits of data to equation 1. Stepping from a potential of −100 to −40 m*V*, K_D increased from 3.9 to 40.6 μM for Kir2.1 and from 65.6 to 170.5 μM for Kir2.4. (*B*) The voltage dependence of the block was assessed by plotting the fractional block against membrane potential at a single Ba^{2+} concentration for Kir2.1, Kir2.4 and HPASM cells. *Solid lines* are the best fit of equation 2. The parameters at a blocking concentration of 100 μM Ba^{2+} were $K_D(0)$ = 142 ± 23 μM, 197 ± 18 μM and 337 ± 45 μM and δ = 0.38 ± 0.04, 0.15 ± 0.02, 0.21 ± 0.03 for Kir2.1 (*n* = 10), Kir2.4 (*n* = 9) and HPASM (*n* = 9) cells, respectively. At 1 mM Ba^{2+}, $K_D(0)$ values were 411.3 ± 89.9 and 1,142 ± 161 μM and δ values were 0.15 ± 0.04 and 0.19 ± 0.06 for Kir2.4 and HPASM, respectively. All data are expressed as mean ± SEM.

recordings (Topert et al., 1998) used this approach to reduce channel open probability in the analysis. We wished to establish if Ba^{2+} has any effect on conductance. Figure 5A shows typical single-channel recordings obtained over a range of potentials from −120 to + 60 m*V* in each experimental condition. The channels all showed strong inward rectification, as indicated by an increased current with membrane hyperpolarization and the lack of channel openings at positive potentials. All channels had a high open probability (Fig. 5B), and this decreased for Kir2.4 in the presence of Ba^{2+}. Similar recordings were obtained in around 20% of HPASM cells, and for Kir2.1 single-channel inward currents were observed at negative membrane potentials in nearly all patches. Kir2.4, due to its high open probability, was less easily identified, with resolvable channel openings being observed in fewer than 5% of cells patched. However, in the presence of Ba^{2+}, the success rate was similar to that of Kir2.1 and records had less background noise. Slope conductances were calculated from the *I-V* relationships (Fig. 5C) and on average were 20.9 ± 0.7 pS (*n* = 6), 19.6 ± 0.5 pS (*n* = 7) and 19.4 ± 1.7 pS (*n* = 4) for HPASM, Kir2.1 and Kir2.4, respectively. For Kir2.4 in the presence of Ba^{2+}, a slope conductance of 22.1 ± 0.9 pS (*n* = 4) was obtained, which was not significantly different from that in the absence of Ba^{2+}. With such similar conductances for all the K_{IR} channels tested, it appears not possible to dissect the molecular components of K_{IR} currents in HPASM cells on the basis of single-channel conductance alone. It should also be noted that inward rectifier channels having conductances between 7 and 35 pS were occasionally observed in HPASM cells, and these may represent either subconductance levels of K_{IR} channels or the existence of distinct populations of channels.

RT-PCR Analysis

RT-PCR analysis of K_{IR} channels was carried out in cultured HPASM cells grown to confluence. PCR was performed in the presence of specific primers for Kir2.1, Kir2.2, Kir2.3 and Kir2.4. Reaction products corresponding to the expected fragment sizes for Kir2.1, Kir2.2 and Kir2.4, but not Kir2.3, were detected in the mRNA from cultured HPASM cells (Fig. 6A). Similar results were obtained in another two experiments. Each of the positive PCR products was confirmed by DNA sequence analysis and found to be correct. A positive control for human Kir2.3 was used to confirm that the primer set used in HPASM cells did indeed give the predicted PCR band (Fig. 6B).

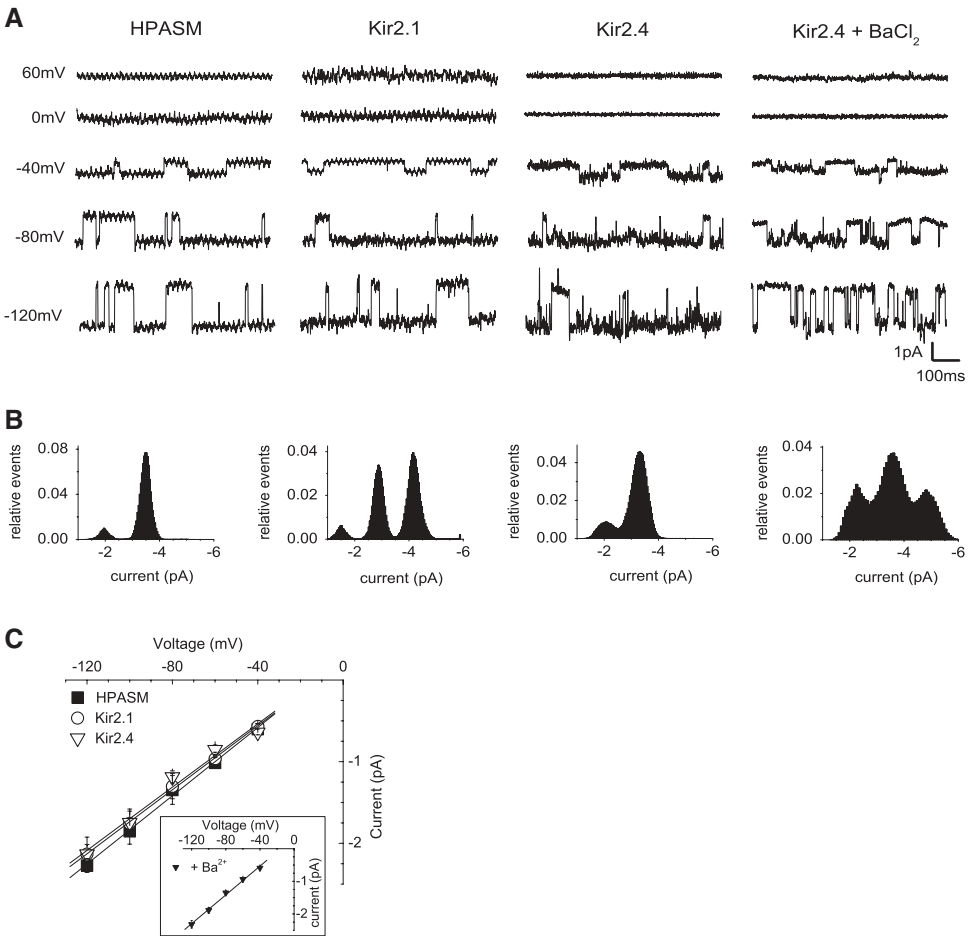

Fig. 5. Single-channel analysis of K_{IR} channels. (*A*) Single unitary events recorded in the cell-attached configuration from a HAPSM cell and HEK-293 cells expressing either Kir2.1 or Kir2.4. Currents, filtered at 500 Hz, were recorded at various test potentials from −120 to + 60 m*V* in symmetrical 140/140 mM K^+, with the closed state indicated. Due to the low frequency of closings with Kir2.4 channels, recordings were also made in the presence of 300 μM $BaCl_2$ in the patch pipette. (*B*) All-points amplitude histograms for recordings shown in *A* at a test potential of −80 m*V* for identical 20-s recordings (0.1 pA bin width). (*C*) Mean single-channel *I-V* relationships recorded in HPASM cells (*closed squares*, $n = 6$) and HEK-293 cells expressing either Kir2.1 (*open circles*, $n = 7$) or Kir2.4 (*open triangles*, $n = 4$), with the *inset* showing recordings in the presence $BaCl_2$ ($n = 5$). Slope conductances were obtained by linear regression, giving values of 20.5 ± 0.9, 19.6 ± 0.9, 19.4 ± 1.7 and 22.0 ± 0.9 pS for HPASM, Kir2.1, Kir2.4 and Kir2.4 in the presence of Ba^{2+}, respectively.

Discussion

K_{IR} channels are expressed in a variety of vascular and visceral smooth muscle tissues. The present study shows for the first time that K_{IR} channels also exist in cultured HPASM cells. This conclusion is based on the following major findings: (1) inward currents showed strong inward rectification and were concentration-dependently blocked by Ba^{2+}, with little effect of this agent on outward currents; (2) the reversal potential of Ba^{2+}-sensitive currents was close to the expected E_K and shifted when external K^+ concentration was altered; (3) RT-PCR analysis confirmed the existence of the Kir2.0 subfamily; and (4) single-channel studies revealed K^+ channel currents with strong inward rectification.

Biophysical Properties of K_{IR} Currents

Within the lung, patch-clamp studies have reported inward currents with rectification strongly dependent on membrane potential and the K^+ gradient in isolated pulmonary artery and vein endothelial cells (Voets et al., 1996; Kamouchi et al., 1997; Michelakis et al., 2001; Hogg et al., 2002; Shimoda et al., 2002), in human bronchial smooth muscle (Snetkov & Ward, 1999; Oonuma et al., 2002) and in human lung cancer cells (Sakai et al., 2002). Similar to that observed in other smooth muscles (Quayle et al., 1997), block by barium is steeply voltage-dependent, increases exponentially with hyperpolarization and takes many milliseconds to develop (Snetkov & Ward, 1999; Sakai et al., 2002; Oonuma et al., 2002).

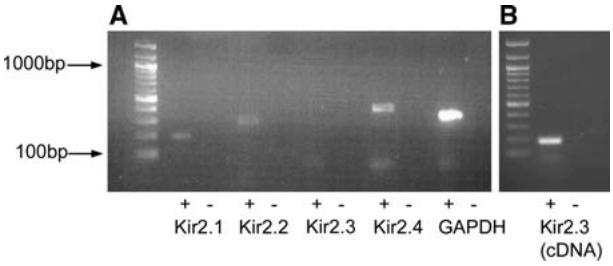

Fig. 6. (*A*) RT-PCR analysis of Kir2.0 subunits in cultured HPASM cells. *Lane 1* contains size makers to indicate the size of the PCR products. Visible products were detected for Kir2.1 (*lane 2*, 199 bp), Kir2.2 (*lane 4*, 269 bp) and Kir2.4 (*lane 8*, 378 bp) but not Kir2.3 (*lane 6*). The reduced form of glyceraldehyde-3-phosphate dehydrogenase (*GAPDH*) was used as a positive control for RT-PCT (*lane 10*). The negative control reactions (absence of reverse transcriptase) were run in lanes 3, 5, 7 and 9. (*B*) Positive control for Kir2.3. *Lane 1* contains size markers, *lane 2* contains positive control product for Kir2.3 (178 bp) and *lane 3* contains reaction with no positive template.

Our results in cultured HPASM cells provide evidence for a K_{IR} current with different characteristics from those previously described in the vasculature or in different types of cultured human lung cells (Voets et al., 1996; Snetkov & Ward, 1999; Sakai et al., 2002; Oonuma et al., 2002). For one, Ba^{2+} block of inward currents showed little time or voltage dependence. This is consistent with Ba^{2+} blocking at a more superficial site within the pore ($\delta = 0.21$) than has previously been described for native K_{IR} currents in vascular smooth muscle (Quayle et al., 1993; Robertson et al., 1996). In these studies, the fraction of the applied electric field sensed by Ba^{2+} was reported to be between 0.51 and 0.55. While we report a δ value in our studies that is slightly lower for Kir2.1 (0.38), if measured using previous methods (K_D values *vs.* membrane potential), this approaches a similar value ($\delta = 0.48$, *data not shown*). The other thing to note was inward currents in HPASM cells were 10- to 30-fold less sensitive to Ba^{2+} than either those we found for cloned mouse Kir2.1 measured under similar conditions or those previously reported for cloned rat Kir2.1 isolated from mesenteric artery (Bradley et al., 1999). In native smooth muscle cells, K_{IR} currents are even more sensitive to Ba^{2+}, where the K_D ranges $\sim 0.4-1$ μM at -100 m*V* (Quayle et al., 1993; Robertson et al., 1996; Oonuma et al., 2002). However, the sensitivity and characteristics of the Ba^{2+} block shown here more closely resembled those of cloned Kir2.4, the only member of the Kir2.0 family to demonstrate low Ba^{2+} sensitivity and weak voltage dependence (Hughes et al., 2000; Liu et al., 2001). It should be noted that in our experiments the Hill coefficient of the sigmoidal fit for Ba^{2+} block in HPASM cells was shallow. The most logical explanation is that whole-cell current contains at least two populations of K_{IR} channels with different Ba^{2+} sensitivities. Indeed, if our data were fitted with a double exponential using slope values obtained from cloned Kir2.1 and Kir2.4, this would give rise to a highly Ba^{2+}-sensitive component contributing about 25% of the total current, with the remainder showing a much lower Ba^{2+} sensitivity (*not shown*). Hetero-multimerization of Kir2.1 and Kir2.4 is also unlikely to explain our data since coexpressing these subunits or a tandem construct resulted not only in currents exhibiting greater sensitivity to Ba^{2+} compared to Kir2.1 alone but also a Hill coefficient of the Ba^{2+} block close to 1 (Schram et al., 2002). The possibility that Kir2.2 contributes to the highly Ba^{2+}-sensitive component, however, remains.

Single-Channel Properties of K_{IR} Channels

Few single-channel recordings of K_{IR} channels have been reported and none to our knowledge in vascular smooth muscle. We successfully recorded single-channel currents corresponding to K_{IR} channels in HPASM cells having single-channel conductances ranging 7–35 pS, with the majority having conductances in the region of 17–22 pS. In heterologous expression systems, single-channel conductances for Kir2.1, Kir2.2, Kir2.3 and Kir2.4 have been reported to be around 20, 35, 10 and 15 pS, respectively, in symmetrical 140 mM K^+ (Topert et al., 1998; Nichols & Lopatin, 1997). In guinea pig ventricular myocytes, at least three types of K_{IR} channels have been reported with mean conductance values of 34.0, 23.8 and 10.7 pS, corresponding most likely to Kir2.2, Kir2.1 and Kir2.3, respectively (Liu et al., 2001). In cultured bovine pulmonary artery endothelial cells, a single-channel conductance of 31 pS was reported in symmetrical 150 mM K^+ (Kamouchi et al., 1997). Kir2.1 was suggested to underlie this channel since molecular data provided no evidence for the existence of Kir2.2. The situation appears somewhat different in human aortic endothelial cells, where unitary conductance distributions showed two prominent peaks around 25 and 35 pS, with the former peak disappearing in the presence of a Kir2.1 dominant negative construct (Fang et al., 2005). So far, the only single-channel data in smooth muscle reports a conductance of 17 pS in cells from human small bronchioles (Snetkov & Ward, 1999), which could correspond to either Kir2.1 or Kir2.4. Likewise, we measured conductances of 20 pS for Kir2.1 and 19 pS for Kir 2.4, suggesting that K_{IR} channels in HPASM cells could correspond to either subunit. It is also worth noting that the presence of Kir2.4 channels could be overlooked in native cells because distinct channel closures were rare unless Ba^{2+} was present in the pipette (*see* Topert et al., 1998). Given the low percentage of patches containing K_{IR} channels in smooth muscle, this could make it difficult to assess the role of Kir2.4, at least at the single-channel level.

Molecular Identity of K_{IR} Channels in Smooth Muscle

So far, the majority of K_{IR} currents described in smooth muscle are likely to be composed of Kir2.1 subunits. Consistent with this, RT-PCR analysis of mRNA showed transcripts for Kir2.1, but not Kir2.2 or Kir2.3, in rat cerebral, mesenteric and coronary arteries (Bradley et al., 1999); canine colon (Flynn et al., 1999); and human bronchial smooth muscle (Oonuma et al., 2002). In cultured human bronchial cells, K_{IR} currents were suppressed by ~75% with antisense oligonucleotides targeted to Kir2.1 mRNA. While such evidence points to a major role of Kir2.1, expression of Kir2.4 was not examined in these studies. In contrast, immunostaining of rat lung sections identified a high level of Kir2.1 expression in arterial and venous endothelial cells but little to none in the smooth muscle layer (Michelakis et al., 2001; Hogg et al., 2002). Interestingly, heterogeneous expression of Kir2.1 was found in the circular muscle layer of the colon, which was associated with a biphasic and differential sensitivity of Ba^{2+} on electrical activity (Flynn et al., 1999). This strongly suggests the existence of more than one K_{IR} conductance; Kir2.4 might be a good candidate since high micromolar Ba^{2+} was required to observe substantial depolarization.

In cultured HPASM cells, we found message for Kir2.1, Kir2.2 and Kir2.4, suggesting whole-cell currents could be made up of a combination of different subunits. Indeed, coexpression of different members of the Kir2.0 subfamily has previously been demonstrated in various tissues. For instance, real-time PCR in rat aortic tissue and human aortic endothelial cells showed that Kir2.2 was the prominent species expressed, followed by Kir2.4 (Alioua et al., 2003; Fang et al., 2005). Kir2.3 and Kir2.1 were also present but less abundant. Furthermore, Kir2.1, Kir2.2 and Kir2.3 were all detected by immunostaining in rat CA1-CA3 pyramidal neurons, granule layer cells of the hippocampus and middle cerebral arteries (Stonehouse et al., 1999). In cardiac myocytes, both Kir2.1 and Kir2.2 appear to be critical components of native K_{IR} current (IK_1), though the relative subunit contribution appears to change from neonatal to adult heart (Nakamura et al., 1999; Liu et al., 2001; Zaritsky et al., 2001). Thus, expression of multiple Kir2.0 subunits appears to be a widespread finding.

Functional Role of K_{IR} Channels

K_{IR} channels have been suggested to play an important role in maintaining resting membrane potential and to be involved in the K^+-induced hyperpolarization of vascular smooth muscle (Edwards et al., 1988; Knot et al., 1996; Quayle, Dart & Standen, 1996; Quayle et al., 1997). In some vessels, K_{IR} channels are the target for endothelium-derived hyperpolarizing factor, where K^+, liberated via endothelial Ca^{2+}-sensitive K^+ channels, is thought to activate K_{IR} channels within the smooth muscle layer (Edwards & Weston, 2004). These channels also appear to underlie relaxation to the stable prostacyclin analogue cicaprost in rat tail artery (Orie, Fry & Clapp, 2006). Genetic manipulation has been employed recently to further clarify the molecular nature of K_{IR} channels and their function in smooth muscle. Using Kir2.1 and Kir2.2 knockout mice, K_{IR} currents were observed in cerebral artery smooth muscle cells isolated from control animals but absent in myocytes from Kir2.1$^{-/-}$ animals (Zaritsky et al., 2000). In addition, the dilator response to K^+ was completely absent in Kir2.1$^{-/-}$, but not Kir2.2$^{-/-}$, animals, suggesting the functional importance of Kir2.1 (Zaritsky et al., 2000). Our data showing Ba^{2+} (100 μM) to significantly depolarize resting membrane potential in cultured HPASM cells suggest that K_{IR} channels do indeed contribute to resting membrane potential in these cells. The relatively high Ba^{2+} required may point to a significant role for Kir2.4. Interestingly, we found that Kir2.4 passed significantly more outward current compared to Kir2.1, making it a good candidate to regulate resting potential in those tissues expressing Kir2.4. However, in view of the fact that changes in gene expression may well occur in culture and alter the electrophysiological properties of HPASM cells (Cui et al., 2002), it remains to be determined whether Kir2.4 contributes to K_{IR} currents in the pulmonary vasculature *in vivo*.

This work was supported by the British Heart Foundation (PG 99176, PG/03/062). L. H. C. is a Medical Research Council Senior Fellow in Basic Science (G117/440).

References

Alioua, A., Conti, L., Eghbali, M., Mahajan, A., Tanaka, Y., Stefani, E., Vandenberg, C., Toro, L. 2003. Inward rectifier K^+ channels (K_{ir}) control muscle tone of a rat conduit vessel: Role of Kir2.x. *Biophys. J.* **84:**225A

Bradley, K.K., Jaggar, J.H., Bonev, A.D., Heppner, T.J., Flynn, E.R.M., Nelson, M.T., Horowitz, B. 1999. $K_{ir}2.1$ encodes the inward rectifier potassium channel in rat arterial smooth muscle. *J. Physiol.* **515:**639–651

Cui, Y., Giblin, J.P., Clapp, L.H., Tinker, A. 2001. A mechanism for ATP-sensitive potassium channel diversity: Functional coassembly of two pore forming subunits. *Proc. Natl. Acad. Sci. USA* **98:**729–734

Cui, Y., Tran, S., Tinker, A., Clapp, L.H. 2002. The molecular composition of K_{ATP} channels in human pulmonary artery smooth muscle cells and their modulation by growth. *Am. J. Respir. Cell. Mol. Biol.* **26:**135–143

Edwards, F.R., Hirst, G.D.S., Silverberg, G.D. 1988. Inward rectification in rat cerebral arterioles: Involvement of potassium ions in autoregulation. *J. Physiol.* **404:**455–466

Edwards, G., Weston, A.H. 2004. Potassium and potassium clouds in endothelium-dependent hyperpolarizations. *Pharmacol. Res.* **49:**535–541

Fang, Y., Schram, G., Romanenko, V.G., Shi, C., Conti, L., Vandenberg, C.A., Davies, P.F., Nattel, S., Levitan, I. 2005. Functional expression of Kir2.x in human aortic endothelial cells: The dominant role of Kir2.2. *Am. J. Physiol.* **289:**C1134–C1144

Flynn, E.R.M., McManus, C.A., Bradley, K.K., Koh, S.D., Hegarty, T.M., Horowitz, B., Sanders, K.M. 1999. Inward rectifier potassium conductance regulates membrane potential of canine smooth muscle. *J. Physiol.* **518:**247–256

Giblin, J.P., Leaney, J.L., Tinker, A. 1999. The molecular assembly of ATP-sensitive potassium channels: Determinants on the pore forming subunit. *J. Biol. Chem.* **274:**22652–22659

Hoger, J.H., Ilyin, V.I., Forsyth, S., Hoger, A. 2002. Shear stress regulates the endothelial Kir2.1 ion channel. *Proc. Natl. Acad. Sci. USA* **99:**7780–7785

Hogg, D.S., McMurray, G., Kozlowski, R.Z. 2002. Endothelial cells freshly isolated from small pulmonary arteries of the rat possess multiple distinct K^+ current profiles. *Lung* **180:**203–214

Hughes, B.A., Kumar, G., Yuan, Y., Swaminathan, A., Yan, D., Sharma, A., Plumley, L., Yang-Feng, T.L., Swaroop, A. 2000. Cloning and functional expression of human retinal Kir2.4, a pH-sensitive inwardly rectifying K^+ channel. *Am. J. Physiol.* **279:**C771–C784

Kamouchi, M., Bremt, K., Eggermont, J., Droogmans, G., Nilius, B. 1997. Modulation of inwardly rectifying potassium channels in cultured bovine pulmonary artery endothelial cells. *J. Physiol.* **504:**545–556

Knot, H.J., Zimmermann, P.A., Nelson, M.T. 1996. External K^+ induced dilations of rat coronary and cerebral arteries involve inward rectifier K^+ channels. *J. Physiol.* **492:**419–430

Liu, G.X., Derst, C., Schlichthorl, G., Heinen, S., Seebohm, G., Bruggemann, A., Kummer, W., Veh, R.W., Daut, J., Preisig-Muller, R. 2001. Comparison of cloned Kir2 channels with native inward rectifier K^+ channels from guinea-pig cardiomyocytes. *J. Physiol.* **532:**115–126

Michelakis, E.D., Weir, E.K., Wu, X., Nsair, A., Waite, R., Hashimoto, K., Puttagunta, L., Knaus, H.G., Archer, S.L. 2001. Potassium channels regulate tone in rat pulmonary veins. *Am. J. Physiol.* **280:**L1138–L1147

Nakamura, T.Y., Lee, K., Artman, M., Rudy, B., Coetzee, W.A. 1999. The role of Kir2.1 in the genesis of native cardiac inward-rectifier K^+ currents during pre- and postnatal development. *Ann. N. Y. Acad. Sci.* **868:**434–437

Nichols, C.G., Lopatin, A.N. 1997. Inward rectifier potassium channels. *Annu. Rev. Physiol.* **59:**171–191

Nilius, B, Droogmans, G. 2001. Ion channels in the vascular endothelium. *Physiol. Rev.* **81:**1415–1459

Oonuma, H., Iwasawa, K., Iida, H., Nagata, T., Imuta, H., Morita, Y., Yamamoto, K., Nagai, R., Omata, M., Nakajima, T. 2002. Inward rectifier K^+ current in human bronchial smooth muscle cells: Inhibition with antisense oligonucleotides targeted to Kir2.1 mRNA. *Am. J. Respir. Cell Mol. Biol.* **26:**371–379

Orie, N.N., Fry, C.H., Clapp, L.H. 2006. Evidence that inward rectifier K^+ channels mediate relaxation by the PGI_2 receptor agonist cicaprost via a cyclic AMP-independent mechanism. *Cardiovasc. Res.* **69:**107–115

Preisig-Muller, R., Schlichthorl, G., Goerge, T., Heinen, S., Bruggemann, A., Rajan, S., Derst, C., Veh, R.W., Daut, J. 2002. Heteromerization of Kir2.x potassium channels contributes to the phenotype of the Andersen's syndrome. *Proc. Natl. Acad. Sci. USA* **99:**7774–7779

Quayle, J.M., Dart, C., Standen, N.B. 1996. The properties and distribution of inward rectifier potassium currents in pig coronary arterial smooth muscle. *J. Physiol.* **494:**715–726

Quayle, J.M., Mccarron, J.G., Brayden, J.E., Nelson, M.T. 1993. Inward rectifier K^+ currents in smooth muscle cells from rat resistance-sized cerebral arteries. *Am. J. Physiol.* **265:**C1363–C1370

Quayle, J.M., Nelson, M.T., Standen, N.B. 1997. ATP-sensitive and inwardly rectifying potassium channels in smooth muscle. *Physiol. Rev.* **77:**1166–1232

Robertson, B.E., Bonev, A.D., Nelson, M.T. 1996. Inward rectifier K^+ currents in smooth muscle cells from rat coronary arteries: Block by Mg^{2+}, Ca^{2+}, and Ba^{2+}. *Am. J. Physiol.* **40:**H696–H705

Sakai, H., Shimizu, T., Hori, K., Ikari, A., Asano, S., Takeguchi, N. 2002. Molecular and pharmacological properties of inwardly rectifying K^+ channels of human lung cancer cells. *Eur. J. Pharmacol.* **435:**125–133

Schram, G., Melnyk, P., Pourrier, M., Wang, Z., Nattel, S. 2002. Kir2.4 and Kir2.1 K^+ channel subunits co-assemble: A potential new contributor to inward rectifier current heterogeneity. *J. Physiol* **544:**337–349

Shimoda, L.A., Welsh, L.E., Pearse, D.B. 2002. Inhibition of inwardly rectifying K^+ channels by cGMP in pulmonary vascular endothelial cells. *Am. J. Physiol.* **283:**L297–L304

Snetkov, V.A., Ward, J.P.T. 1999. Ion currents in smooth muscle cells from human small bronchioloes: Presence of an inward rectifier K^+ current and three types of large conductance K^+ channels. *Exp. Physiol.* **84:**835–846

Stanfield, P.R., Nakajima, S., Nakajima, Y. 2002. Constitutively active and G-protein coupled inward rectifier K^+ channels: Kir2.0 and Kir3.0. *Rev. Physiol. Biochem. Pharmacol.* **145:**47–179

Stonehouse, A.H., Pringle, J.H., Norman, R.I., Stanfield, P.R., Conley, E.C., Brammar, W.J. 1999. Characterisation of Kir2.0 proteins in the rat cerebellum and hippocampus by polyclonal antibodies. *Histochem. Cell Biol.* **112:**457–465

Topert, C., Doring, F., Wischmeyer, E., Karschin, C., Brockhaus, J., Ballanyi, K., Derst, C., Karschin, A. 1998. Kir2.4: A novel K^+ inward rectifier channel associated with motoneurons of cranial nerve nuclei. *J. Neurosci.* **18:**4096–4105

Voets, T., Droogmans, G., Nilius, B. 1996. Membrane currents and the resting membrane potential in cultured bovine pulmonary artery endothelial cells. *J. Physiol.* **497:**95–107

Woodhull, A.M. 1973. Ionic blockage of sodium channels in nerve. *J. Gen. Physiol* **61:**687–708

Zaritsky, J.J., Eckman, D.M., Wellman, G.C., Nelson, M.T., Schwarz, T.L. 2000. Targeted disruption of Kir2.1 and Kir2.2 genes reveals the essential role of the inwardly rectifying K^+ current in K^+-mediated vasodilation. *Circ. Res.* **87:**160–166

Zaritsky, J.J., Redell, J.B., Tempel, B.L., Schwarz, T.L. 2001. The consequences of disrupting cardiac inwardly rectifying K^+ current (I_{K1}) as revealed by the targeted deletion of the murine Kir2.1 and Kir2.2 genes. *J. Physiol.* **533:**697–710